

UAV-VLPA*: A Vision-Language-Path-Action System for Optimal Route Generation on a Large Scales

Oleg Sautenkov
Skoltech
Moscow, Russia

oleg.sautenkov@skoltech.ru

Aibek Akhmetkazy*
Skoltech
Moscow, Russia

aibek.akhmetkazy@skoltech.ru

Yasheerah Yaqoot*
Skoltech
Moscow, Russia

yasheerah.yaqoot@skoltech.ru

Muhammad Ahsan Mustafa
Skoltech
Moscow, Russia

ahsan.mustafa@skoltech.ru

Grik Tadevosyan
Skoltech
Moscow, Russia
grik.tadevosyan@skoltech.ru

Artem Lykov
Skoltech
Moscow, Russia
artem.lykov@skoltech.ru

Dzmitry Tsetseroukou
Skoltech
Moscow, Russia
d.tsetseroukou@skoltech.ru

Abstract—The UAV-VLPA* (Visual-Language-Planning-and-Action) system represents a cutting-edge advancement in aerial robotics, designed to enhance communication and operational efficiency for unmanned aerial vehicles (UAVs). By integrating advanced planning capabilities, the system addresses the Traveling Salesman Problem (TSP) to optimize flight paths, reducing the total trajectory length by 18.5% compared to traditional methods. Additionally, the incorporation of the A* algorithm enables robust obstacle avoidance, ensuring safe and efficient navigation in complex environments. The system leverages satellite imagery processing combined with the Visual Language Model (VLM) and GPT’s natural language processing capabilities, allowing users to generate detailed flight plans through simple text commands. This seamless fusion of visual and linguistic analysis empowers precise decision-making and mission planning, making UAV-VLPA* a transformative tool for modern aerial operations. With its unmatched operational efficiency, navigational safety, and user-friendly functionality, UAV-VLPA* sets a new standard in autonomous aerial robotics, paving the way for future innovations in the field.

Index Terms—VLA; VLM; LLM-agents; VLM-agents; UAV; Navigation; Drone; Path Planning.

I. INTRODUCTION

The field of aerial robotics has advanced significantly, with unmanned aerial vehicles (UAVs) becoming crucial in various applications, including surveillance, agriculture, and disaster management [1]. As UAV missions grow more complex, the need for effective path planning and autonomous mission generation has become increasingly important. Traditional UAV control methods typically rely on manual waypoint navigation or basic pre-programmed paths [2], [3], which are often labor-intensive and require specialized knowledge to operate effectively. However, as missions become more dynamic and environments more complex, these traditional methods are no

* These authors contributed equally to this work.

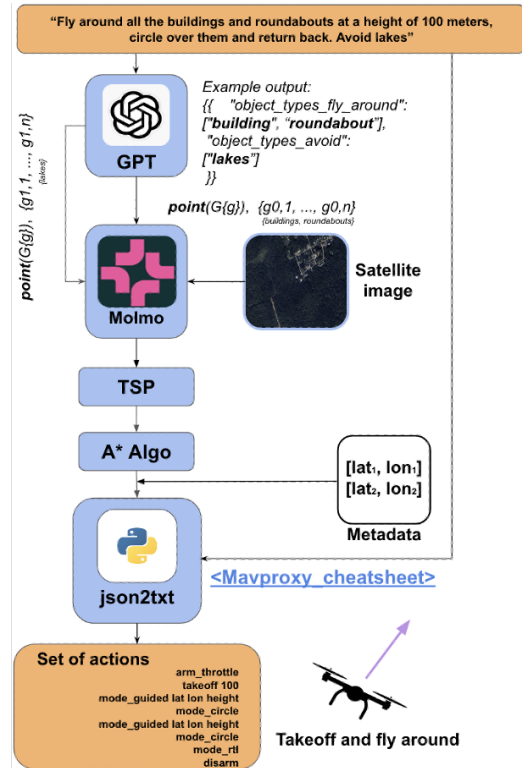


Fig. 1: The pipeline of the UAV-VLPA system.

longer sufficient, and more intelligent systems are needed for efficient and autonomous mission planning.

In recent years, Vision-Language-Action (VLA) and Vision-Language-Navigation (VLN) systems have emerged as an innovative solution, enabling UAVs to autonomously navigate

from natural language instructions [4], [5], [6], [7]. These systems are based on transformer models that interpret natural language inputs and, in some cases, use satellite data to plan and execute missions [7]. Building upon the UAV-VLA framework [4], which generates actionable paths from linguistic instructions and satellite images, this paper extends the system by incorporating the Traveling Salesman Problem (TSP) into the mission generation process to ensure optimal path planning.

Leveraging the language request, we focus on introducing path planning for UAVs by integrating obstacle avoidance techniques with TSP for optimal route generation. The objective is to reduce mission completion time and minimize trajectory length while ensuring safe navigation through environments with potential obstacles. Using the outputs of the UAV-VLPA* system, we apply TSP to optimize the routes, taking into account environmental constraints and minimizing errors in path execution. This enables the UAV to generate more efficient paths that avoid obstacles while ensuring mission objectives are met.

The integration of satellite data into the UAV-VLPA* system significantly enhances its capabilities, as such data is widely accessible and open globally. By utilizing open satellite data alongside real-time environmental information, the system can improve the accuracy and adaptability of path planning and obstacle avoidance. This combination allows for more informed decision-making, enabling UAVs to navigate complex environments with greater precision and efficiency. The use of open satellite data not only enriches the system’s contextual understanding but also ensures cost-effective and scalable solutions for diverse aerial missions.

We use the benchmark **UAV-VLPA-nano-30** [4] to evaluate the performance of our system, demonstrating that the integration of TSP with obstacle-aware path planning results in improved mission execution, outperforming human-level performance in large-scale UAV missions. Our contributions are as follows:

- We introduce the **UAV-VLPA*** framework, combining Vision-Language based Path Planning with the Traveling Salesman Problem and Path Planning for optimal route generation.
- We apply obstacle avoidance using A* algorithm in the mission generation process to ensure safe and efficient UAV navigation in complex environments.
- We demonstrate that our integrated system, outperforms human-level path planning in large-scale UAV mission scenarios.

II. RELATED WORK

The introduction of Vision Transformers (ViT) [8], [9] marked a significant advancement in the development of full-fledged models capable of processing and integrating multiple types of input and output, including text, images, video, and more. Building on this progress, the leading companies introduced models like ChatGPT-4 Omni [10] and DeepSeek R1 [11], which can reason across audio, vision, and text in real

time, enabling seamless multimodal interactions. To address the problem of objects finding in robotics applications, Allen Institute of AI introduced model Molmo, that can point the requested objects on an image [12].

The usage of the transformer-based models allowed the extensive developing of the new methods, benchmarks, and datasets for Vision Language Navigation and Vision Language Action tasks. Firstly, the problem of Aerial Visual Language Navigation was proposed by Liu et al. [13], where they introduced the Aerial VLN method together with AerialVLN dataset. In [7] Fan et al. described the simulator and VLDN system, that can support the dialog with an operator during the flight. Lee et al. [5] presented an extended dataset with geographical meta information (streets, squares, boulevards, etc.). The introduction of dataset was paired with the new approach for goal predictor. Zhang et al. [14] took a pioneering step by building a universal environment for embodied intelligence in an open city. The agents there can perform both VLA and VLN tasks together online. Gao et al. [15] presented a method, where a map was provided as a matrix to the LLM model. In that work was introduced the Semantic Topo Metric Representation (STMR) approach, that allowed to feed the matrix map representation into the Large Language Model. In [16] Wang et al. presented the benchmark and simulator dubbed OpenUAV platform, which provides realistic environments, flight simulation, and comprehensive algorithmic support.

Google DeepMind introduced the RT-1 model in their study [17], wherein the model generates commands for robot operation. The researchers collected an extensive and diverse dataset over several months to train the model. Utilizing this dataset, they developed a transformer-based architecture capable of producing 11-dimensional actions within a discrete action space. Building on the foundation of RT-1, the subsequent RT-2 model [18] integrates the RT-1 framework with a Visual-Language Model, thereby enabling more advanced multimodal action generation in robotic systems. The work of [19], [20], and [21] highlights the potential of transformers and end-to-end neural networks to handle complex Vision-Language-Action (VLA) tasks in real time.

III. SYSTEM OVERVIEW

Originally, the Visual Language Model (VLM) provided outputs by identifying point objects on an image in a sequential manner, from left to right and top to bottom, without considering obstacles or their spatial relationships. To address these limitations, we propose the following steps.

A. System Workflow

- **Instruction parsing, Vision-Language Processing, and Waypoint Generation:** We process the instruction to identify and extract target objects for visitation and obstacles for avoidance. The VLM detects and points obstacles (e.g., buildings) while also interpreting any textual restrictions if they are. As the result, a comprehensive list of waypoints and prohibited regions is produced based on the VLM outputs.

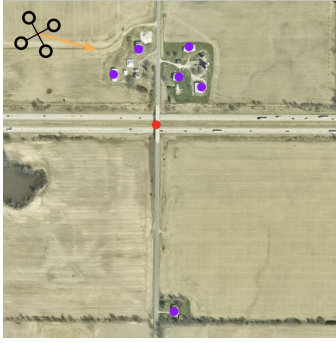


Fig. 2: The Waypoint Generation

- **TSP Route Construction:** A local search heuristic (2-opt) [22] is used to build an initial route that covers all waypoints efficiently.

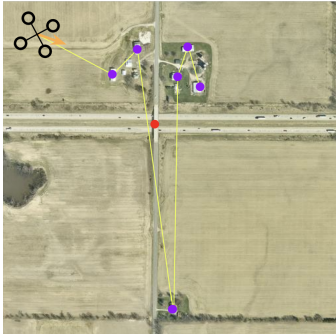


Fig. 3: The 2-Opt Local TSP Search

- **A* Path Refinement:** A* then refines each leg of the TSP solution to navigate around obstacles. If necessary, the route is iteratively updated to ensure feasibility.

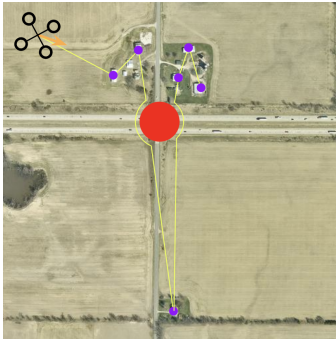


Fig. 4: The A* algorithm

- **Final Path Output:** The optimized and obstacle-free route is passed to the post-processing part of the pipeline.

B. Traveling Salesman Problem

The TSP-based component of our system is used to minimize the total travel distance by identifying an optimal or near-optimal tour through a predefined set of waypoints. To achieve this, we implement local search heuristics, specifically the 2-opt scheme [22], which iteratively refines candidate tours to

enhance their efficiency. The local search process begins with an initial permutation of waypoints and generates neighboring solutions by systematically swapping pairs of edges. The search continues until no further improvements can be made, at which point the solution converges to a local minimum. It is important to note that this local minimum depends on the specific perturbation scheme employed and may not necessarily coincide with the global minimum. This step ensures that the generated route optimally covers all required waypoints in terms of distance, while detailed obstacle constraints are addressed in subsequent stages.

C. Path Planning and Obstacle Avoidance

To efficiently execute the A* algorithm in large-scale environments, the map is discretized into a uniform grid of equally sized cells, where each cell represents a node in the graph. The grid resolution is determined by balancing path fidelity—how accurately the path adheres to real-world terrain and obstacles—and computational efficiency—the number of nodes processed during the search. In this work, the discretization step is set to 5 pixels.

- **Grid Creation:** The continuous 2D area is subdivided into $\Delta x \times \Delta y$ cells. For each cell, we check whether it is traversable (i.e., not blocked by an obstacle) based on obstacle data extracted from VLM.
- **Coordinate System Mapping:** Each cell is assigned a discrete coordinate pair (i, j) corresponding to its row (i) and column (j) indices.
- **Traversability Check:** During grid creation, any cell that intersects with a detected obstacle (e.g., a lake) is marked as non-traversable. Such cells are effectively removed from the final graph so that the A* search will not expand them.

Another significant reason for selecting this algorithm is its computational efficiency. The algorithm exhibits a time complexity of

$$O(E \log(V)) \quad (1)$$

and a space complexity of

$$O(V) \quad (2)$$

where E represents the number of edges and V denotes the number of vertices in the constructed graph. These efficiency characteristics make the algorithm highly suitable for large-scale applications, ensuring optimal performance in terms of both computational time and memory usage.

D. Path Planning and Obstacle Avoidance with Traveling Salesman Problem

To exploit both the global optimization property of TSP and the obstacle-avoidance capability of A*, we introduce a hybrid approach. The TSP solution identifies a minimal traversal order among all waypoints, while A* is integrated on each leg of the TSP tour to avoid obstacles. By combining these methods, we ensure that the route remains both globally efficient and locally safe in the presence of uncertain or densely packed by obstacles environments.

IV. EXPERIMENTAL SETUP

The system was evaluated using the command: “*Create a flight plan for the quadcopter to fly around each building at a height of 100 m, return to home, and land at the take-off point. Avoid lakes*”. The experiment was conducted on a PC with an RTX 4090 graphics card (24GB VRAM) and Intel Core i9-13900K processor. Due to memory constraints, the quantized Molmo-7B-D BnB 4-bit model [23] was used.

V. EXPERIMENTAL RESULTS

A. Results with only TSP

To evaluate the impact of the Traveling Salesman Problem (TSP) on the UAV-VLA system, we applied TSP to the UAV-VLPA-nano-30 benchmark. The total trajectory length generated by the system was 51.34 km, which is significantly shorter than the trajectory length from the human-generated flight paths, which was 63.89 km, as reported in the UAV-VLA paper [4]. The manual flight plans used in the UAV-VLA paper are consistent with the results presented here, and only the TSP optimization was implemented, resulting in a reduction of the trajectory length from 77.74 km to 51.34 km.

The performance of the system was further evaluated using various error metrics, including KNN error, DTW RMSE, and Interpolation RMSE [4]. The results are summarized in Table I:

TABLE I. COMPARISON OF RMSE METRICS FOR DIFFERENT METHODS ON UAV-VLA WITH TSP

Metric (RMSE)	KNN (m)	DTW (m)	Sequential (m)
Mean	45.1586	259.066	354.463
Median	26.8865	235.483	308.907
Max	336.22	719.478	734.317

Additionally, we present two key plots to visualize the trajectory length comparison and the error analysis. Fig. 5 shows the comparison of trajectory lengths generated by the UAV-VLA system [4] with TSP and by an experienced operator, highlighting the efficiency gains when applying TSP. Fig. 6 illustrates the error distribution of the UAV-VLA system with TSP in comparison with ground truth, showing the performance of the system across different error metrics.

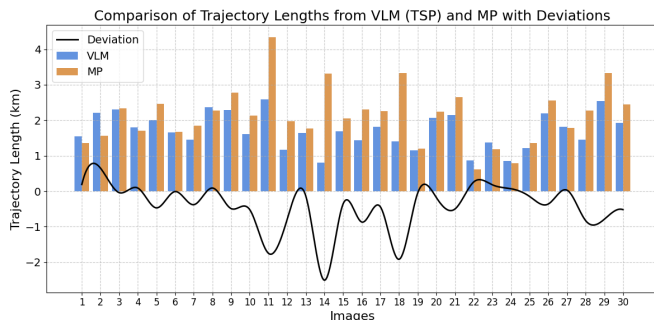


Fig. 5: The comparison of the trajectory lengths made by UAV-VLA with TSP and by an experienced operator.

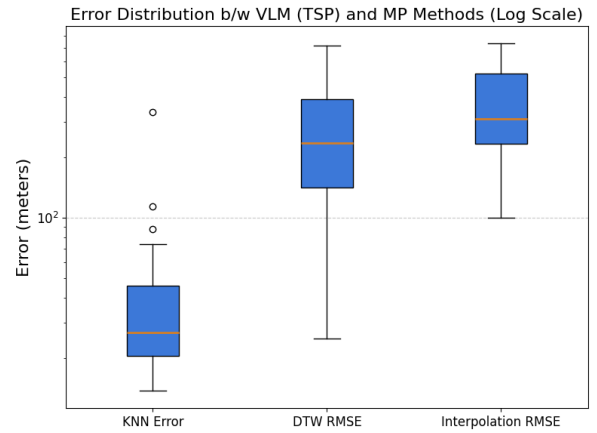


Fig. 6: The error of UAV-VLA with TSP in comparison with ground truth.

The results demonstrate that integrating TSP with the UAV-VLA system significantly enhances the efficiency of UAV path planning, reducing trajectory lengths while maintaining high performance across error metrics.

B. Results with the A* path planning algorithm

For this and next sections human-made path was changed due to additional requirement of avoiding the lakes on images. That’s why total trajectory length and mission construction time were slightly changed.

The total trajectory length generated by the system with A* path planning only was 76.84 km, which is significantly longer than the trajectory length from the human-generated flight paths, which was 62.95 km.

Trajectory length comparison and the error analysis are shown in figures below. Fig. 7 shows the comparison of trajectory lengths generated by the UAV-VLA system with path planning application and by an experienced operator.

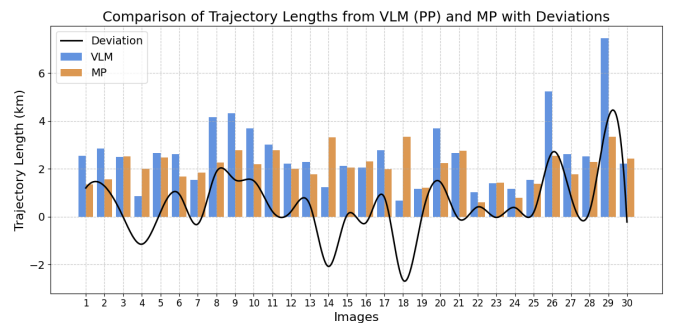


Fig. 7: The comparison of the trajectory lengths made by UAV-VLA with A* path planning algorithm and by an experienced operator.

The system performance was also evaluated the same as in the TSP only section V-A. The results are summarized and shown in Table II:

Error distribution of the system across different error metrics is drawn in Fig. 8.

TABLE II. COMPARISON OF RMSE METRICS FOR DIFFERENT METHODS ON UAV-VLA WITH PATH PLANNING

Metric (RMSE)	KNN (m)	DTW (m)	Sequential (m)
Mean	70.1541	262.675	403.305
Median	53.6504	267.013	366.284
Max	337.358	534.32	730.027

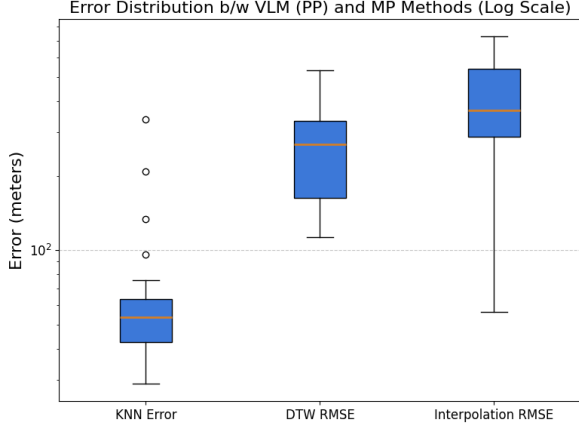


Fig. 8: The error of UAV-VLA with A* path planning algorithm in comparison with ground truth.

Flight comparison of the Human-made path and the path created by VLM and A* algorithm only is shown in the Fig. 9

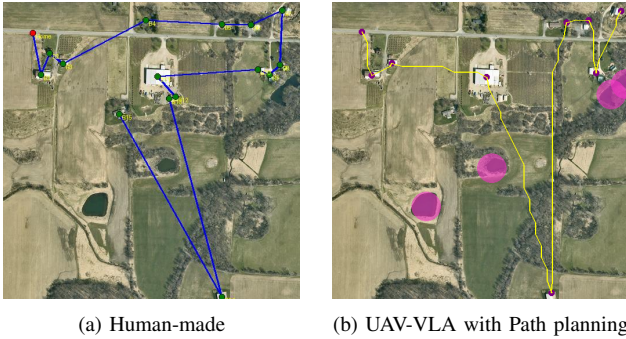


Fig. 9: Comparison of flight plans generated by a **human expert** (a) and the UAV-VLA with **Path planning only** system (b).

C. Results with TSP and A* Path Planning

The total trajectory length generated by the system with A* path planning and TSP (UAV-VLPA system) only was 51.27 km, which is shorter than the trajectory length from the human-generated flight paths, which was equal to 62.95 km. The system performance was also evaluated similarly to the TSP only and Path planning only sections. The results are summarized and shown in Table III:

Trajectory length comparison and the error analysis are shown in figures below. Fig. 10 shows the comparison of trajectory lengths generated by the UAV-VLA system with path planning application and by an experienced operator.

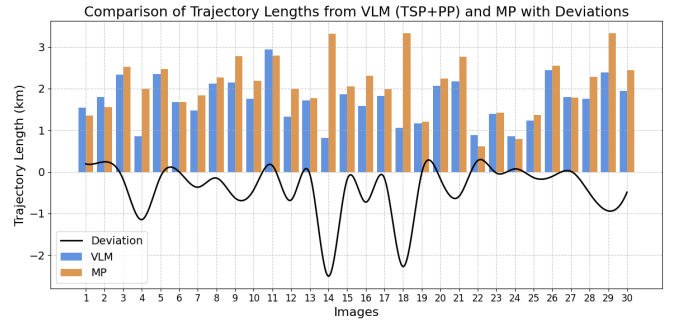


Fig. 10: The comparison of the trajectory lengths made by the UAV-VLPA system and by an experienced operator.

TABLE III. COMPARISON OF RMSE METRICS FOR DIFFERENT METHODS ON THE UAV-VLPA SYSTEM

Metric (RMSE)	KNN (m)	DTW (m)	Sequential (m)
Mean	69.1918	223.936	348.24
Median	54.4354	170.953	291.855
Max	337.886	476.072	723.488

Error distribution of the system across different error metrics is drawn in Fig. 11. Example of the path created by the UAV-VLPA system is shown in Fig. 12.

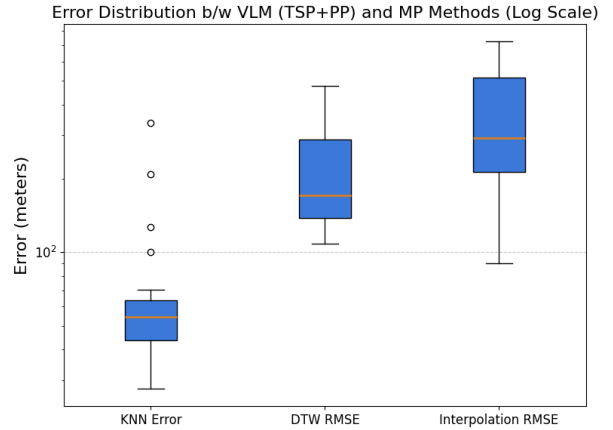


Fig. 11: The error distribution of the UAV-VLPA system in comparison with ground truth.

VI. CONCLUSION

Application of the Vision-Language Model and Traveling Salesman Problem Method significantly increases the speed of the large mission generation. Overall mission generation time for VLM was 11 times less and total trajectory length for TSP-Path planning was 24.4% shorter than in the human-made missions. **22/30** or 73.3% TSP-Path planning trajectories were shorter than the human-made ones. The Implementation of the Traveling Salesman Problem resulted in a reduction of the trajectory length from 77.74 km to 51.34 km.

When applying the A* algorithm directly to raw data, the resulting path distance increases by 22%. This clearly

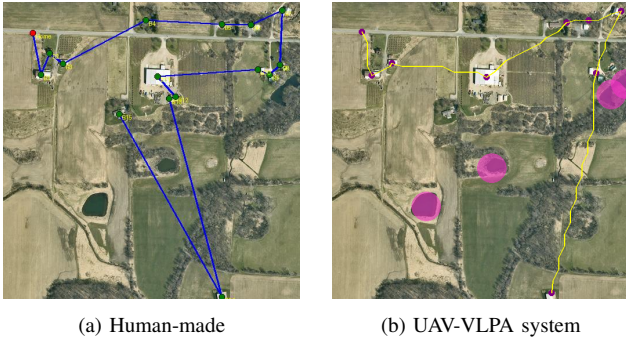


Fig. 12: Comparison of flight plans generated by a human expert (a) and the UAV-VLPA system (b).

demonstrates the inefficiency of using unprocessed data for path planning.

The integration of the TSP approach followed by A* path-planning resulted in an overall trajectory reduction of 18.5% compared to human-generated paths. Additionally, the system demonstrated superior performance, achieving the shortest path in 25 out of 30 test cases. This highlights the effectiveness of the combined approach in optimizing path planning and reducing travel distance. Furthermore, the system's ability to consistently outperform human-generated paths underscores its potential for practical applications in autonomous navigation and mission planning.

VII. FUTURE WORK

The integration of global path planning through language requests represents a transformative tool for future applications in autonomous systems. By leveraging open satellite data alongside classical mathematical approaches, such as the Traveling Salesman Problem (TSP) and A* algorithm, we can unlock powerful opportunities for optimizing navigation in complex environments. Future work will focus on enhancing the system's ability to process real-time satellite imagery and dynamically adapt to changing environmental conditions, further improving path accuracy and efficiency.

REFERENCES

- [1] J. Su, X. Zhu, S. Li, and W.-H. Chen, "AI meets UAVs: A survey on AI empowered UAV perception systems for precision agriculture," *Neurocomputing*, vol. 518, pp. 242–270, 2023.
- [2] O. Sautenkov, S. Asfaw, Y. Yaqoot, M. A. Mustafa, A. Fedoseev, D. Trinitatova, and D. Tsetsrukou, "FlightAR: AR Flight Assistance Interface with Multiple Video Streams and Object Detection Aimed at Immersive Drone Control," *arXiv preprint arXiv:2410.16943*, 2024.
- [3] G. Tadevosyan, M. Osipenko, D. Aschu, A. Fedoseev, V. Serpiva, O. Sautenkov, S. Karaf, and D. Tsetsrukou, "Safeswarm: Decentralized safe rl for the swarm of drones landing in dense crowds," 2025. [Online]. Available: <https://arxiv.org/abs/2501.07566>
- [4] O. Sautenkov, Y. Yaqoot, A. Lykov, M. A. Mustafa, G. Tadevosyan, A. Akhmetkazy, M. A. Cabrera, M. Martynov, S. Karaf, and D. Tsetsrukou, "UAV-VLA: Vision-Language-Action System for Large Scale Aerial Mission Generation," *arXiv preprint arXiv:2501.05014*, 2025.
- [5] J. Lee, T. Miyanishi, S. Kurita, K. Sakamoto, D. Azuma, Y. Matsuo, and N. Inoue, "CityNav: Language-Goal Aerial Navigation Dataset with Geographic Information," *arXiv preprint arXiv:2406.14240*, 2024.

- [6] J. Zhong, M. Li, Y. Chen, Z. Wei, F. Yang, and H. Shen, "A Safer Vision-based Autonomous Planning System for Quadrotor UAVs with Dynamic Obstacle Trajectory Prediction and Its Application with LLMs," *arXiv preprint arXiv:2311.12893*, 2023.
- [7] Y. Fan, W. Chen, T. Jiang, C. Zhou, Y. Zhang, and X. E. Wang, "Aerial Vision-and-Dialog Navigation," *arXiv preprint arXiv:2205.12219*, 2023.
- [8] A. Dosovitskiy, L. Beyer, A. Kolesnikov, D. Weissenborn, X. Zhai, T. Unterthiner, M. Dehghani, M. Minderer, G. Heigold, S. Gelly, T. Uszkoreit, and N. Houlsby, "An Image is Worth 16x16 Words: Transformers for Image Recognition at Scale," *arXiv preprint arXiv:2010.11929*, 2021.
- [9] A. Radford, J. W. Kim, C. Hallacy, A. Ramesh, G. Goh, S. Agarwal, G. Sastry, A. Askell, P. Mishkin, J. Clark, G. Krueger, and I. Sutskever, "Learning Transferable Visual Models from Natural Language Supervision," *arXiv preprint arXiv:2103.00020*, 2021.
- [10] OpenAI *et al.*, "GPT-4 Technical Report," *arXiv preprint arXiv:2303.08774*, 2024.
- [11] DeepSeek, "Deepseek: A large language model for natural language processing," <https://www.deepseek.com>, 2023, accessed: 31-Jan-2025.
- [12] M. Deitke *et al.*, "Molmo and PixMo: Open Weights and Open Data for State-of-the-Art Multimodal Models," *arXiv preprint arXiv:2409.17146*, 2024.
- [13] S. Liu, H. Zhang, Y. Qi, P. Wang, Y. Zhang, and Q. Wu, "AerialVLN: Vision-and-Language Navigation for UAVs," *arXiv preprint arXiv:2308.06735*, 2023.
- [14] W. Zhang, Y. Liu, X. Wang, X. Chen, C. Gao, and X. Chen, "Embodied-City: Embodied Aerial Agent for City-level Visual Language Navigation Using Large Language Model," in *2024 23rd ACM/IEEE International Conference on Information Processing in Sensor Networks (IPSN)*, 2024, pp. 265–266.
- [15] Y. Gao, Z. Wang, L. Jing, D. Wang, X. Li, and B. Zhao, "Aerial Vision-and-Language Navigation via Semantic-Topo-Metric Representation Guided LLM Reasoning," *arXiv preprint arXiv:2410.08500*, 2024.
- [16] X. Wang, D. Yang, Z. Wang, H. Kwan, J. Chen, W. Wu, H. Li, Y. Liao, and S. Liu, "Towards Realistic UAV Vision-Language Navigation: Platform, Benchmark, and Methodology," *arXiv preprint arXiv:2410.07087*, 2024.
- [17] A. Brohan *et al.*, "RT-1: Robotics Transformer for Real-World Control at Scale," *arXiv preprint arXiv:2212.06817*, 2023.
- [18] A. Brohan, N. Brown *et al.*, "RT-2: Vision-Language-Action Models Transfer Web Knowledge to Robotic Control," *arXiv preprint arXiv:2307.15818*, 2023.
- [19] M. J. Kim, K. Pertsch, S. Karamcheti, T. Xiao, A. Balakrishna, S. Nair, R. Raffailov, E. Foster, G. Lam, P. Sanketi, Q. Vuong, T. Kollar, B. Burchfiel, R. Tedrake, D. Sadigh, S. Levine, P. Liang, and C. Finn, "OpenVLA: An Open-Source Vision-Language-Action Model," *arXiv preprint arXiv:2406.09246*, 2024.
- [20] O. X.-E. Collaboration and A. O'Neill, "Open X-Embodiment: Robotic learning datasets and RT-X models," <https://arxiv.org/abs/2310.08864>, 2023.
- [21] K. F. Gbagbe, M. A. Cabrera, A. Alabbas, O. Alyunes, A. Lykov, and D. Tsetsrukou, "Bi-VLA: Vision-Language-Action Model-Based System for Bimanual Robotic Dexterous Manipulations," *arXiv preprint arXiv:2405.06039*, 2024.
- [22] P. R. de O. da Costa, J. Rhuggenaath, Y. Zhang, and A. Akcay, "Learning 2-opt heuristics for the traveling salesman problem via deep reinforcement learning," 2020. [Online]. Available: <https://arxiv.org/abs/2004.01608>
- [23] *Molmo-7B-D BnB 4bit quantized 7GB*, 2024. [Online]. Available: <https://huggingface.co/cyan2k/molmo-7B-D-bnb-4bit>